Quaternary Science Reviews 142 (2016) 90–101

Contents lists available at ScienceDirect

Quaternary Science Reviews

journal homepage: www.elsevier.com/locate/quascirev

Relative sea-level change in northeastern Florida (USA) during the last ~8.0 ka

Andrea D. Hawkes [a, *], Andrew C. Kemp [b], Jeffrey P. Donnelly [c], Benjamin P. Horton [d, e], W. Richard Peltier [f], Niamh Cahill [g], David F. Hill [h], Erica Ashe [i, j], Clark R. Alexander [k]

[a] Department of Geography and Geology, University of North Carolina Wilmington, Wilmington, NC 28403, USA
[b] Department of Earth and Ocean Sciences, Tufts University, Medford, MA 02155, USA
[c] Geology and Geophysics, Woods Hole Oceanographic Institution, Woods Hole, MA 02543, USA
[d] Institute of Marine Science and Coastal Sciences, Rutgers University, New Brunswick, NJ 08901, USA
[e] Division of Earth Sciences, Earth Observatory of Singapore, Nanyang Technological University, 639798, Singapore
[f] Department of Physics, University of Toronto, Toronto, Ontario, Canada
[g] School of Mathematical Sciences (Statistics), Complex Adaptive Systems Laboratory, University College Dublin, Dublin 4, Ireland
[h] School of Civil and Construction Engineering, Oregon State University, Corvallis, OR 97331, USA
[i] Department of Statistics and Biostatistics, Rutgers University, Piscataway, NJ 08854, USA
[j] CCICADA (Command, Control, and Interoperability Center for Advanced Data Analysis, A Department of Homeland Security Center of Excellence), USA
[k] Skidaway Institute of Oceanography, The University of Georgia, Savannah, GA 31411, USA

ARTICLE INFO

Article history:
Received 18 January 2016
Received in revised form
14 April 2016
Accepted 18 April 2016

Keywords:
Salt marsh
Holocene
Foraminifera
Georgia
St. Marys River

ABSTRACT

An existing database of relative sea-level (RSL) reconstructions from the U.S. Atlantic coast lacked valid sea-level index points from Georgia and Florida. This region lies on the edge of the collapsing forebulge of the former Laurentide Ice Sheet making it an important location for understanding glacio-isostatic adjustment and the history of ice-sheet melt. To address the paucity of data, we reconstruct RSL in northeastern Florida (St. Marys) over the last ~8.0 ka from samples of basal salt-marsh sediment that minimize the influence of compaction. The analogy between modern salt-marsh foraminifera and their fossil counterparts preserved in the sedimentary record was used to estimate paleomarsh surface elevation. Sample ages were determined by radiocarbon dating of identifiable and *in-situ* plant macrofossils. This approach yielded 25 new sea-level index points that constrain a ~5.7 m rise in RSL during the last ~8.0 ka. The record shows that no highstand in sea level occurred in this region over the period of the reconstruction. We compared the new reconstruction to Earth-ice models ICE 6G-C VM5a and ICE 6G-C VM6. There is good fit in the later part of the Holocene with VM5a and for a brief time in the earlier Holocene with VM6. However, there are discrepancies in model-reconstruction fit in the early to mid Holocene in northeastern Florida and elsewhere along the Atlantic coast at locations with early Holocene RSL reconstructions. The most pronounced feature of the new reconstruction is a slow down in the rate of RSL rise from approximately 5.0 to 3.0 ka. This trend may reflect a significant contribution from local-scale processes such as tidal-range change and/or change in base flow of the St. Marys River in response to paleoclimate changes. However, the spatial expression (local vs. regional) of this slow down is undetermined and corroborative records are needed to establish its geographical extent.

1. Introduction

On passive margins such as the Atlantic coast of North America, regional-scale relative sea-level (RSL) change during the Holocene was primarily driven by the balance between eustatic and isostatic processes (e.g. Clark et al., 1978; Farrell and Clark, 1976). This balance evolved through time and varied among regions, resulting in distinctive patterns and trends of Holocene RSL change that shed light on the driving mechanisms causing past, present, and future RSL change at regional to global scales. In particular, RSL reconstructions provide empirical data for testing and parameterizing Earth-ice models, which are assumed to be accurate when

* Corresponding author.
E-mail address: hawkesa@uncw.edu (A.D. Hawkes).

http://dx.doi.org/10.1016/j.quascirev.2016.04.016
0277-3791/

they are used (for example) to correct measurements made by tide gauges and satellites to isolate climate-driven sea-level trends (e.g. Peltier and Tushingham, 1991), or to identify likely sources of paleo-meltwater input to the global ocean (e.g. Liu et al., 2016; Mitrovica et al., 2011). Additionally, regional RSL histories provide an important constraint on interpretations of coastal geomorphology and a paleo-environmental context for the interpretation of archaeological remains (e.g. DePratter and Thompson, 2013; Turck and Alexander, 2013). However, RSL reconstructions from a single site inherently include the influence of local-scale factors such as tidal-range change (e.g. Hall et al., 2013) and sediment compaction (e.g. Kaye and Barghoorn, 1964) that can cause differences from the prevailing regional trend.

Along the U.S. Atlantic coast, Engelhart and Horton (2012) compiled and standardized Holocene RSL reconstructions produced from salt-marsh sediment to describe trends in 16 regions between Maine and South Carolina. This dataset represents a latitudinal gradient away from the Laurentide Ice Sheet and differing RSL trends among regions reflect the spatially-variable contribution of glacio-isostatic adjustment (GIA). However, there was an absence of valid sea-level index points from Georgia and Florida (Fig. 1A). The southeastern U.S Atlantic coast is an important region because it lies on the edge of the collapsing forebulge that is distal to the former ice sheet making it sensitive to forebulge geometry and an important region for testing Earth-ice models. Furthermore, this region is a geographic link between efforts to compile Holocene RSL reconstructions from North America (Engelhart and Horton, 2012) and the Caribbean (e.g. Milne and Peros, 2013; Toscano and Macintyre, 2003) that would enable the geometry of the collapsing forebulge to be better resolved by empirical data that span the transition from high to near zero rates of GIA (Khan et al., 2015). The lack of data from Florida and Georgia has also prevented resolution to a long-running debate about the occurrence of a Holocene highstand (sea-level above present) in the southeastern United States (e.g. Froede, 2002; Wanless, 1982; Scholl and Stuiver, 1967; Scott et al., 1995).

To address the paucity of Holocene RSL reconstructions from northeastern Florida we produced 25 new sea-level index points spanning the period from ~8.0 to 2.0 ka using foraminifera preserved in radiocarbon-dated salt-marsh sediment. The reconstructions were developed from basal salt-marsh sediment to minimize the influence of compaction and were standardized to allow direct comparison with existing reconstructions from elsewhere. The multi-millennial pattern of RSL rise in northeastern

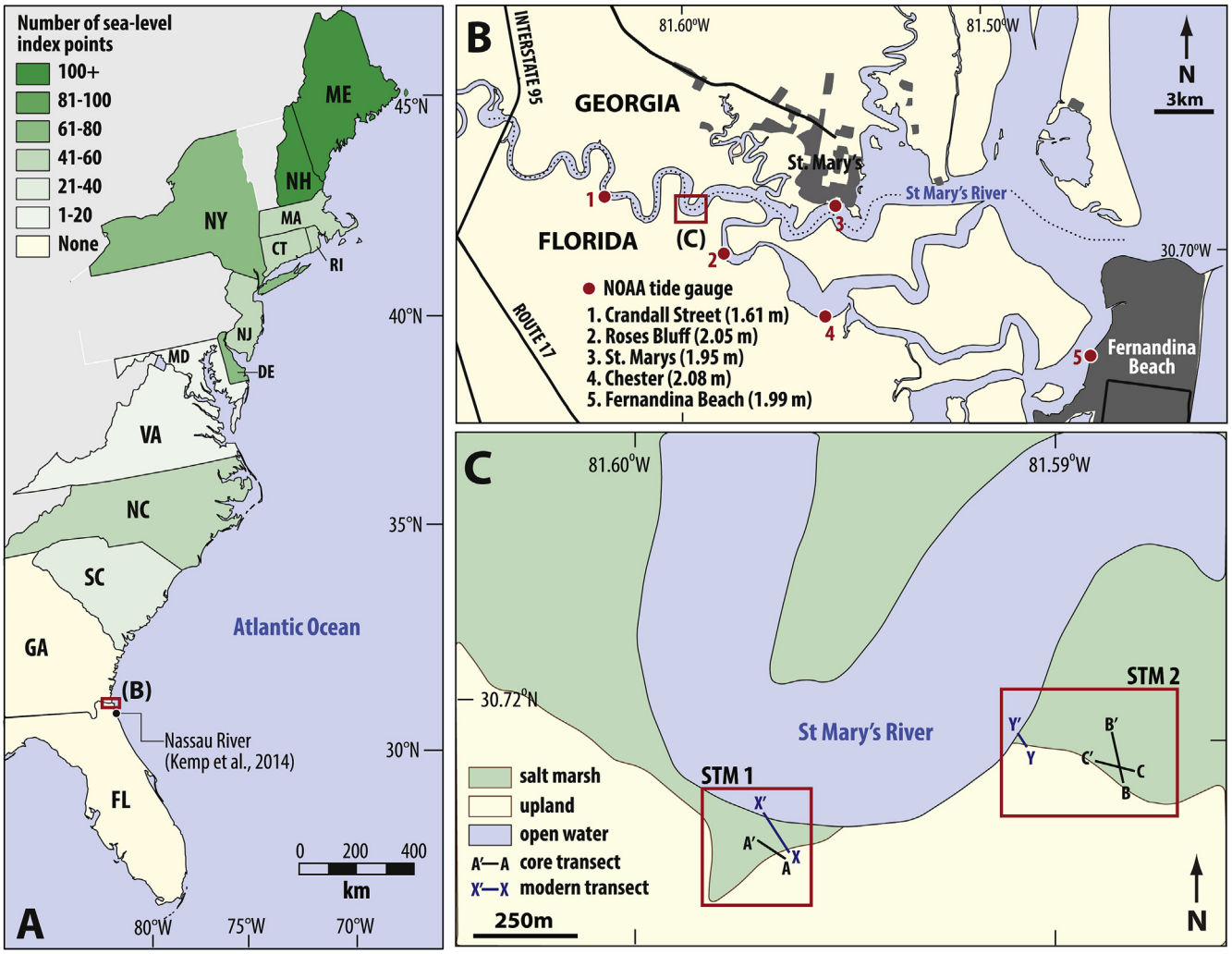

Fig. 1. **(A)** The spatial distribution of sea-level index points along the U.S. Atlantic coast by state from Engelhart and Horton (2012) indicating the lack of data for Georgia and Florida. An existing reconstruction from Nassau Landing (Kemp et al., 2014) was used to generate ten sea-level index points spanning the last ~2500 years. **(B,C)** Location of the STM 1 and STM 2 study sites in the St. Marys River in northeastern Florida. Location of NOAA-operated tide gauges on the St. Marys River are shown with great diurnal tidal range listed for each station.

Florida displays the characteristic pattern of collapse of the Laurentide Ice Sheet's proglacial forebulge and includes no evidence for the occurrence of a Holocene highstand. However, a plateau in the RSL reconstruction at ~5.5–2.0 ka is not a feature of predictions from the ICE-6G_C VM6 Earth-ice model or RSL reconstructions from nearby regions and may represent an unexplained, regional signal over a restricted latitudinal range, or an important contribution from local-scale processes at the St. Marys site.

2. Study site

The St. Marys River forms part of the border between Florida and Georgia (Fig. 1). It is often called a blackwater river because of its dark coloring from tannins introduced to the river as it flows through freshwater peat bogs in the Okefenokee Swamp and salt marshes in its tidal reaches. Salt-marshes along the river form a narrow, low-marsh zone occupied by tall-form *Spartina alterniflora* that is characterized by muddy sediment. The monotypic, high-marsh zone is vegetated by *Juncus roemerianus* and characterized by peat formation. The transition from salt-marsh to forested, freshwater upland environments is often unvegetated because over-hanging canopy keeps these areas shaded. The sediment accumulating in this zone is black, amorphous, and organic.

Our study site on the St. Marys River is comprised of two adjacent areas of salt marsh (STM 1 and STM 2; Fig. 1) that were chosen for detailed analysis after exploratory coring at many locations in the estuary showed that these sites had the deepest and thickest accumulations of salt-marsh sediment. The great diurnal tidal range (mean lower low water, MLLW, to mean higher high water, MHHW) in the St. Marys River decreases with distance up estuary from 2.00 m at Fernandina Beach and 2.04 m at Roses Bluff, to 1.61 m at the Crandall Street tide gauge (Fig. 1B). We estimated the local tidal prism (great diurnal tidal range of 2.00 m) at the study site using the VDatum transformation tool from NOAA. The maximum cumulative uncertainty reported for VDatum in coastal waters and inland waterways in the Florida/Georgia region is ±0.10 m (1σ), and includes uncertainty with benchmarks in the study area. Since no estimate of the elevation of High Astronomical Tide (HAT) is provided by the nearest tide gauges (Roses Bluff and Crandall Street) we estimated it as occurring at 25% of the great diurnal tidal range above MHHW (1.52 m above mean tide level, MTL). This estimate is from HAT values reported at Fernandina Beach and the same approach was used by Kemp et al. (2014) in the nearby Nassau River estuary.

3. Methods

3.1. Modern foraminifera

We used surface (0–1 cm) sediment samples collected along two transects (one at STM 1 and one at STM 2; Fig. 1C) to characterize the modern distribution of foraminifera in salt-marsh environments on the St. Marys River. The transects ran from unvegetated, tidal-flat environments, through the low-marsh and high-marsh zones, and into the freshwater upland forest. Samples were positioned along each transect at regular vertical increments to ensure that all plant zones were included. The samples were stored in buffered ethanol and stained with rose Bengal to enable live and dead individuals to be distinguished from one another (Walton, 1952). Prior to counting, each sample was washed over stacked 63 μm and 500 μm sieves to isolate foraminfera-bearing sediment. A minimum of 100 dead individuals were enumerated under a binocular microscope from a sub-sample of the original sediment, if fewer than 100 dead individuals were present the entire sample was counted. All species of the genus *Ammobaculites* were combined into a single group because of the difficulty of identifying frequently broken individuals to the species level. All species of the genus *Haplophragmoides* were combined into a single group. In each instance the combined species occupy the same range of tidal elevations and are characteristic of the same salt-marsh sub enviornments and we conclude that our taxonomy has no discernible influence on the resulting RSL reconstruction (e.g., Edwards and Wright, 2015; Wright et al., 2011).

3.2. Sediment cores

At STM 1 and STM 2, we collected cores of basal sediment along the prevailing subsurface gradient that separated taupe-colored, consolidated Pleistocene sand from the overlying organic, salt-marsh sediment. Each core was collected using a Russian corer to prevent compaction and/or contamination during sampling. Individual, 50-cm long cores were positioned to include the contact between basal sand and overlying organic sediment. Cores were positioned relative to one another in order to sample the basal contact at approximately equal changes in elevation from −5.23 m to +0.46 m NAVD88 (North American Vertical Datum of 1988). Each core was transferred to a rigid plastic sleeve, wrapped in plastic, and stored under refrigerated conditions until analyzed. We used Real Time Kinematic (RTK) satellite navigation to establish a temporary benchmark at site STM 1 and also at STM 2. Core-top (and surface sample) elevations were referenced to these points by leveling with a total station. We estimated a leveling uncertainty of ±0.11 m at STM 1 and ±0.05 m at STM 2 based on reported RTK performance. Conversion from NAVD88 to local tidal datums was achieved using the VDatum transformation tool.

In the laboratory each core was processed by using one half to identify material suitable for radiocarbon dating and by preparing the other half for foraminiferal analysis. Radiocarbon dating was limited to material that we recognized as being deposited on a paleo marsh surface such as fragments of leaves or bark found lying horizontally in the cores, or the identifiable rhizomes of short-lived salt-marsh plants that grew close to the former marsh surface. All samples sent for radiocarbon dating were first cleaned under a binocular microscope to remove contaminating material such as younger roots and adhered sediment. They were then oven dried at ~45 °C and submitted to the National Ocean Sciences Accelerator Mass Spectrometry facility for dating where they underwent standard acid-base-acid pretreatment and $\delta^{13}C$ was measured directly on an aliquot of CO_2 collected during sample combustion. Reported radiocarbon ages were individually calibrated using the Intcal13 dataset (Reimer et al., 2013) and we used the upper and lower 2σ calibrated ages as the range of possible ages for the dated sample. Samples for foraminiferal analysis were prepared following the method described for surface samples, with the exception of staining. Beginning at the visible, basal contact between Pleistocene sand and Holocene organic sediment, we analyzed successive samples upcore to identify the position where foraminifera appeared in sufficient abundance (at least 30 individuals) to determine that the assemblage could reasonably be interpreted as being *in situ*. The first sample with a viable assemblage of foraminifera and material suitable for radiocarbon dating was used to produce a sea-level index point from each core. In a small number of cores, adjacent samples were radiocarbon dated as check on the reliability and consistency of ages derived from plant macrofossils that could be allocthonous (e.g. leaves and bark). We counted foraminifera in additional core samples surrounding the dated level to ensure that it was representative of the prevailing environmental conditions at the time of sediment deposition.

3.3. Relative sea-level reconstruction

We followed the standardized approach described in Engelhart and Horton (2012) to produce sea-level index points that estimate the unique position of former sea level in time and space with uncertainty. The vertical position of a sea-level index point (i.e. the height of RSL) is established using a proxy that is commonly called a sea-level indicator. Geomorphic features, geochemical properties of sediments, and biological assemblages can be sea-level indicators if their observable distribution in modern coastal environments is limited to the intertidal zone, or a specific part of it (e.g. Shennan et al., 2015). Salt-marsh plants and foraminifera (e.g. Edwards and Wright, 2015; Scott and Medioli, 1978) are sea-level indicators because their tolerances and preferences for tidal inundation vary among species and result in a characteristic pattern of vertical zonation, where the assemblage occupying one part of a salt-marsh is different to those at a different tidal elevation. The indicative meaning defines the range of tidal elevations over which a particular sea-level indicator forms (Woodroffe and Barlow, 2015). It is comprised of a mid-point called the reference water level and the difference in height between the upper and lower elevation of the sea-level indicator is termed the indicative range. RSL is reconstructed through reasoning by analogy, where paleo sea-level indicators are assigned a reference water level and indicative range based on their similarity to modern equivalents, whose distribution was established through systematic observations.

In their standardized compilation of RSL reconstructions, Engelhart and Horton (2012) treated low salt-marsh zones as forming at elevations between MTL and mean high water (MHW), while they treated high salt-marsh zones as existing from MHW to HAT. This model of ecological zonation is common across climate and salt-marsh floral zones on the Atlantic coast of North America (e.g. Adams, 1963; Johnson and York, 1915; Mckee and Patrick, 1988; Redfield, 1972) and is appropriate for use in salt marshes in northeastern Florida (e.g. Pomeroy and Wiegert, 1981; Wiegert and Freeman, 1990).

Foraminifera preserved in core samples of coastal sediment at STM 1 and STM 2 were used as sea-level indicators by classifying them as having formed in either a low or high salt-marsh environment and by considering the sedimentary context and character of the sample. In keeping with the approach of Engelhart and Horton (2012), this classification relied on researcher judgement rather than a statistical method. We used the modern transects from St. Marys to identify the species of foraminifera that occupy and characterize modern low and high salt-marsh environments in the study region. Consequently, RSL was calculated using the following equation;

$$RSL = E_i - RWL_i \quad (1)$$

where E_i is the elevation of the sample i measured as depth in a core whose top was leveled to local tidal datums and RWL_i is the reference water level assigned to sample i on the basis of foraminifera preserved in the sample and its sedimentary context. Both quantities are expressed relative to the same tidal datum such that E_i and RWL_i are equal for a surface sample and RSL today is 0 m. The E_i term is subject to uncertainties associated with sampling such as leveling errors and sample thickness. The uncertainty of the RWL_i term is the indicative range of the sea-level indicator being used. These sources of error were combined using the following equation;

$$E_i = \sqrt{[e_1^2 + e_2^2 + \ldots e_n^2]} \quad (2)$$

where E_i is the total vertical error estimated for sample i and $e_1 \ldots e_n$ are the individual sources of error. We used the 2σ calibrated age range from radiocarbon dating as the sample age. This approach inherently assumes that tidal range was unchanged through time.

Each sea-level index point was classified to reflect its relative susceptibility to sediment compaction.

Base of basal sea-level index points are derived from salt-marsh sediment lying less than 5 cm above an incompressible substrate (Pleistocene sand at St. Marys) and are considered to be free from the effects of sediment compaction. Basal index points lie within the same sedimentary unit that overlies the incompressible substrate, but are located more than 5 cm above the contact. These samples may have experienced some compaction.

3.4. Relative sea-level trends

Collections of sea-level index points constrain the evolution of RSL in time and space. To quantitatively describe RSL trends in northeastern Florida during the Holocene we combined the new sea-level index points from St. Marys with ten others from the nearby Nassau River estuary (Fig. 1A; Kemp et al., 2014). These additional sea-level index points span the last ~2.5 ka and were included after applying the same standardized approach to ensure consistency among records. We analyzed the combined RSL record for northeastern Florida using the Errors-In-Variables Integrated Gaussian Process (EIV-IGP) model of Cahill et al. (2015). This model formally accounts for the unique combination of vertical and temporal uncertainties of individual sea-level index points and also the uneven distribution of sea-level index points through time by using two well-known statistical approaches. Firstly, the EIV approach (Dey et al., 2000) accounts for age uncertainty arising from radiocarbon dating of the sediment cores. Secondly, the Gaussian process approach (Rasmussen and Williams, 2005) is useful for modeling the non-linear RSL data. A Gaussian process is fully specified by a mean function (set to zero) and a covariance function that relates the sea-level index points to one another. The EIV-IGP model places a Gaussian-process prior on the rate of RSL change through time (the rate process). The mean of the likelihood for the sea-level index points is estimated by integrating the rate process (Cahill et al., 2015).

4. Results

4.1. Modern distribution of foraminifera

At site STM 1 we collected 19 surface sediment samples along a transect that extended from +1.33 m to −0.74 m MTL (Fig. 2). The transect spanned a freshwater upland forest (stations 1 and 2), a zone of unvegetated black organic sediment in the shade of the overhanging forest (stations 3–8), a mono-specific, high salt marsh vegetated by *J. roemerianus* (stations 9–14), a narrow low salt-marsh zone of tall-form *Spartina alterniflora* (stations 15–17), and an unvegetated tidal flat (stations 18 and 19). Foraminifera were absent from the samples collected in the forest at elevations above 0.97 m MTL. Within the black, amorphous organic sediment *Haplophragmoides* spp. (up to 59%) and *Trochammina inflata* (up to 38%) were the most abundant species of foraminifera at elevations from 0.64 m to 0.97 m MTL. *Jadammina macrescens* was commonly present in this zone (5–25%). The zones of *J. roemerianus*, tall-form *S. alterniflora*, and the tidal flat were characterized by relatively high abundances of *Ammoastuta inepta* (average 13%) and *Miliammina fusca* (average 25%) and variable occurrences of *Ammobaculites* spp. (0–21%). This assemblage extended down to an elevation of at least −0.74 m MTL.

The transect at STM 2 was positioned to capture a different high

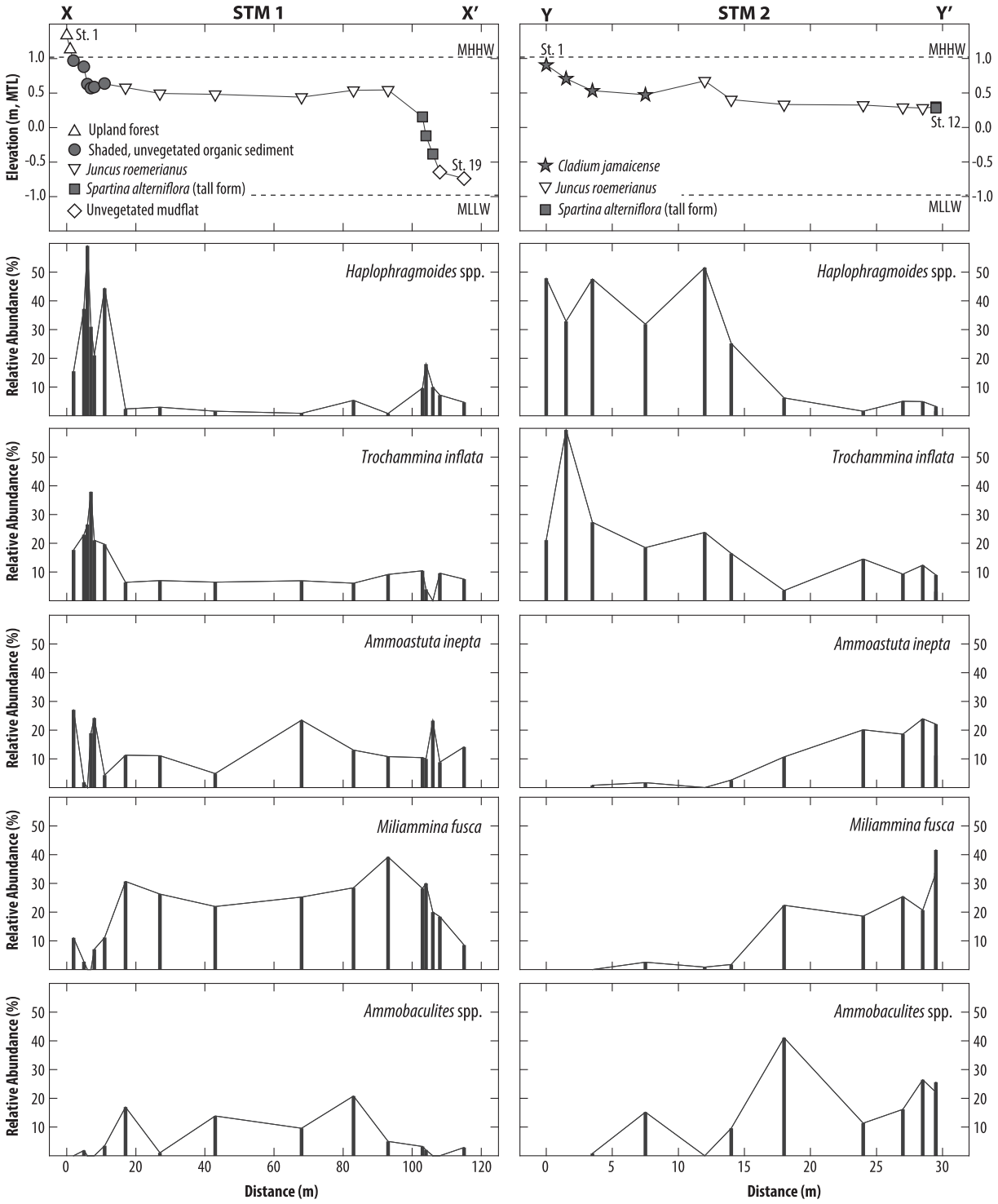

Fig. 2. Distribution of modern foraminifera along transects from tidal flat, low salt-marsh, high salt-marsh and freshwater upland vegetation zones at sites STM 1 (left panels) and STM 2 (right panels). MHHW = mean higher high water, MLLW = mean lower low water, MTL = mean tide level. Shaded symbols denote the dominant type of vegetation at each sampling station.

salt-marsh plant community than was present at STM 1 because of a lack of overhanging canopy. The transect comprised 12 surface sediment samples from +0.91 m to +0.28 m MTL (Fig. 2) and included vegetation zones dominated by *Cladium jamaicense* (stations 1–4), *J. roemerianus* (stations 5–10), and tall-from *S. alterniflora* (stations 11 and 12). Foraminifera were present in all samples. The peat-forming environments at stations 1–6 were characterized by high abundances of *Haplophragmoides* spp. (average 40%) and *T. inflata* (average 28%). *J. macrescens* (up to 27%) was also an important part of this assemblage. *A. inepta* (up to 24%), *M. fusca* (up to 42%), and *Ammobaculites* spp. (up to 41%) became increasingly abundant at lower elevations. Modern foraminiferal data are presented in Appendix A.

4.2. Sea-level index points

At site STM 1, the contact between basal sand and the overlying organic sediment was sampled at locations along a ~45 m transect and across a range of elevations from −1.76 m NAVD88 (core 5) to 0.46 m NAVD88 (core T6; Fig. 3). The most abundant foraminifera preserved in core samples were *Haplophragmoides wilberti*, *Arenoparrella mexicana*, *Tiphotrocha comprimata* and *A. inepta*. These benthic, agglutinated and predominantly epifaunal species are typical of high salt-marsh environments in the southeastern United States (e.g. Goldstein and Frey, 1986; Kemp et al., 2009) and at the St Marys site (Fig. 2) where these enviornments are comprised of fine-grained, highly organic sediment and brackish to normal salinity. The absence of characteristic low-marsh species such as *M. fusca* and/or *Ammobaculites* spp. reinfornces this interpretation. Coupled with sediment texture described in the field (peat including, in some instances, the preserved remains of identifiable high salt-marsh plants), these assemblages indicate deposition in a high salt-marsh environment and we therefore assigned them an indicative range of MHW to HAT. Foraminifera were present within 5 cm of the basal contact in all radiocarbon-dated cores. In cores 1, 2, 4, 7, and 8 sea-level index points were not produced, either because elevations were repetitious of other cores, or foraminifera were sparse or absent. Nine of the radiocarbon dates were from fragments of single leaves found lying horizontal in the cores indicating deposition on a paleo marsh surface. In many instances

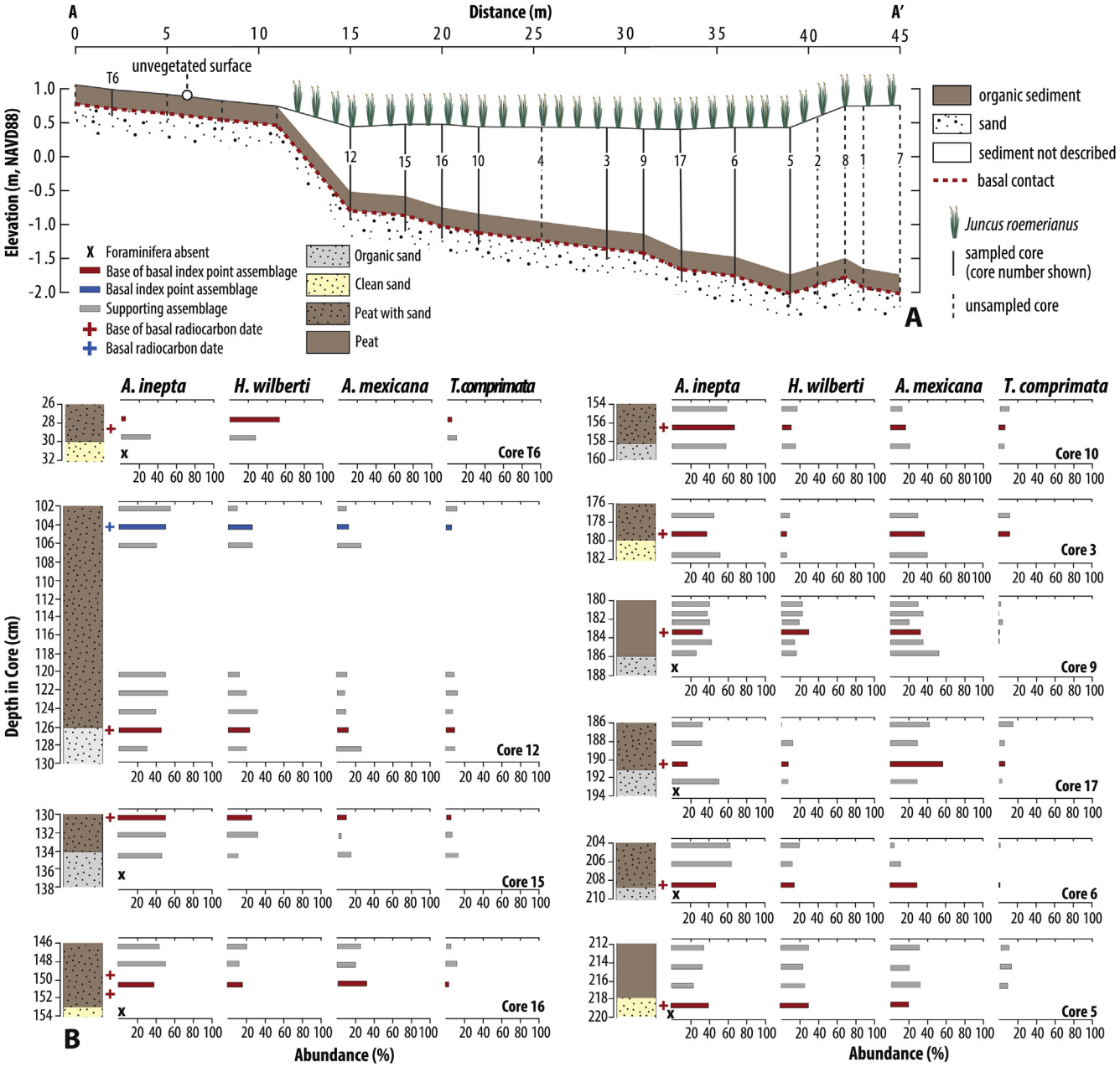

Fig. 3. Cores and samples used to develop sea-level index points at STM 1. **(A)** Position of sampled cores along a transect used to describe the contact between basal sand and the overlying organic units. **(B)** Lithology of individual cores and foraminifera enumerated from 1-cm thick samples, only the most common four species are shown. Colored bars represent the foraminiferal data used to infer the environment of deposition for producing sea-level index points. The position of radiocarbon-dated material is also shown. (For interpretation of the references to color in this figure legend, the reader is referred to the web version of this article.)

the veination and stem of the leaf was preserved, suggesting that individual macrofossils were unlikely to have been transported over long periods of time before being incorporated into the sedimentary record. The remaining three dates were from a *J. roemerianus* rhizome, a woody fragment, and a piece of bark that we interpreted as having grown *in situ* (rhizome) or been deposited on a paleomarsh surface (wood fragment and bark) from the nearby upland. These cores yielded 11 base of basal sea-level index points and one basal sea-level index point, which show that RSL at STM 1 rose from approximately −2.0 m at 3.6 ka to −0.5 m at 0.3 ka.

At site STM 2 we reconstructed RSL using sediment cores collected along two transects (B–B′ and C–C′; Fig. 1C). Transect B–B′ (~130 m long; Fig. 4) included six sediment cores that sampled the contact between basal sand and overlying organic sediment across an elevational range from −5.23 m NAVD88 (core 17) to −2.36 m NAVD88 (core 4). The basal sediment was comprised of peat or peat with sand and included several species of high salt-marsh foraminifera (including *H. wilberti*, *A. mexicana*, and *J. macrescens*). Therefore, we ascribed the samples an indicative range of MHW to HAT when reconstructing RSL. Radiocarbon dates were from woody fragments (six), bark (one), and reed parts (two) that we interpret as having been deposited on the marsh surface. These cores yielded two base of basal sea-level index points and seven basal sea-level index points than ranged in age from approximately 4.0 ka to 7.8 ka (Fig. 4). Other cores were not used to reconstruct RSL because they were not from unique elevations and/or did not preserve foraminifera in sufficient numbers (>30 individuals) to make a reliable paleoenvironmental interpretation (cores 2, 6, 8). STM 2 transect C–C′ (~65 m long; Fig. 5) included four sediment cores that sampled the contact between basal sand and overlying organic sediment across an elevational range from −3.66 m NAVD88 (core 10) to −4.08 m NAVD88 (core 13). These samples were dominated by high salt-marsh foraminifera and were assigned an indicative range of MHW to HAT. Four radiocarbon dates, two on plant fragments, one on a reed stem, and one on a horizontal leaf produced two base of basal sea-level index points and two basal sea-level index points between 6.0 ka and 6.8 ka (Fig. 5). Cores 7 and 14 were not used to produce index sea-level index points either because elevations were repetitious of other cores, or foraminifera were sparse or absent. Combined, transects B and C produced 13 sea-level index points including four base of basal samples and nine basal samples. At STM 2 RSL rose from approximately −6.3 m at 7.8 ka to −3.5 m at 4.0 ka. The details of all sea-level index points produced at STM1 and STM 2 (including radiocarbon ages) are presented in Appendix B.

4.3. Relative sea-level trends

The 25 new sea-level index points from St. Marys show that RSL rose from approximately −6.3 m at 7.8 ka to −0.5 m at 0.3 ka (Fig. 6). The St Marys index points were combined with data from the Nassau River estuary (~15 km south of St Marys, Fig. 1A; Kemp et al., 2014) to produce a RSL reconstruction spanning the period since ~7.8 ka with a greater density of sea-level index points in the late Holocene than was possible using the St Marys reconstruction alone. The Nassau River reconstruction is comprised of 10 radiocarbon-dated samples of high salt-marsh peat with abundant *J. roemerianus* macrofossils in which *A. inepta* was the dominant species of foraminifera. To ensure comparability among records, we standardized the Nassau River reconstruction using the approach applied at St Marys and in the U.S. Atlantic coast database of Engelhart and Horton (2012). There are three time points when sea-level index points from both St Marys and Nassau River are available (Fig. 6B). There is agreement between reconstructions from the two sites at ~0.4 ka and ~2.3 ka as evidenced by the significant overlap of sea-level index points within their uncertainties. At ~2.5 ka there is only marginal overlap between sea-level index points from St Marys and Nassau River, possibly indicating local-scale differences between the two sites at this time. However, the general agreement between the two sites and the late Holocene RSL trends that they record, supports our decision to combine the reconstructions into a single record.

An EIV-IGP model was fitted to the combined dataset of RSL reconstructions from St. Marys and Nassau River to describe trends through time (Fig. 6B) with quantitative consideration of the unique temporal and vertical uncertainties of each sea-level index point and their uneven distribution through time (the model treats data from St. Marys and Nassau River as a single location). The resulting RSL curve shows continuous rise during the last ~7.8 ka and no evidence for RSL higher than present at any time during this interval. There was an overall decrease in the rate of RSL rise since ~7.8 ka, but a plateau in the RSL curve at approximately 5.0 ka to 3.0 ka resulted in the rate of RSL rise falling to a minimum of 0.35 mm/a (−0.23–0.96 mm/a 95% credible interval) at ~4.1 ka (Fig. 6C). It subsequently rose to 1.17 mm/a (0.67–1.66 mm/a 95% credible interval) at ~2.3 ka before decreasing continuously. For comparison, the linear rate of RSL rise measured by the Fernandina Beach tide gauge (Fig. 1B) since 1897 CE is 2.05 mm/a (Fig. 6C).

5. Discussion

5.1. Comparison to Earth-ice models

The standardized database of Holocene RSL reconstructions from the U.S. Atlantic coast (Engelhart and Horton, 2012) provided important empirical data to test and refine Earth-ice models because it spanned much of the Holocene and consisted of regional-scale reconstructions at increasing distance from the former center of the Laurentide Ice Sheet. By comparing RSL reconstructions to a suite of Earth-ice models for 16 regions, Engelhart et al. (2011) recognized that the ICE 5G VM5a model misfit RSL reconstructions in regions south of Maine, with the difference being largest in the mid-Atlantic and southeastern United States. Substituting the ICE 6G model for ICE 5G resulted in minimal changes to predicted RSL in regions south of the former ice margin of Long Island, but resulted in greater coherence between modeled and reconstructed RSL in the northeastern United States except Maine. Changing the Earth model from VM5a to VM5b (decreased upper mantle viscosity) increased the fit to RSL reconstructions for regions south of Massachusetts. However, the models examined by Engelhart et al. (2011) continued to predict RSL considerably lower than was reconstructed in regions including, and further south than, North Carolina for the period prior to ~5 ka. Roy and Peltier (2015) developed a new Earth model (VM6) that was coupled with a revised ice model (ICE 6G-C; Argus et al., 2014; Peltier et al., 2015), which significantly improved the fit between model predictions and RSL reconstructions. For data older than 4.0 ka the improvement was particularly pronounced south of the Delaware Estuary.

We generated RSL predictions for St. Marys using the ICE 6G-C VM5a and ICE 6G-C VM6 models to investigate how well they fit the new reconstruction (Fig. 6B). For the period since ~8.0 ka both Earth-ice models predict a continuous, but decelerating RSL rise at St. Marys. The ICE 6G-C VM6 model shows RSL of −3.91 m at 6 ka compared to −6.74 m for ICE 6G-C VM5a. At 4 ka the difference between model predictions of RSL is reduced to 1.84 m and is 0.79 m at 2 ka (Peltier et al., 2015; Roy and Peltier, 2015). Since 4.0 ka the ICE 6G-C VM5a model provides a better fit to the RSL reconstruction than the ICE 6G-C VM6 model. Prior to 4.0 ka there is little consistency among Earth-ice model predictions and the

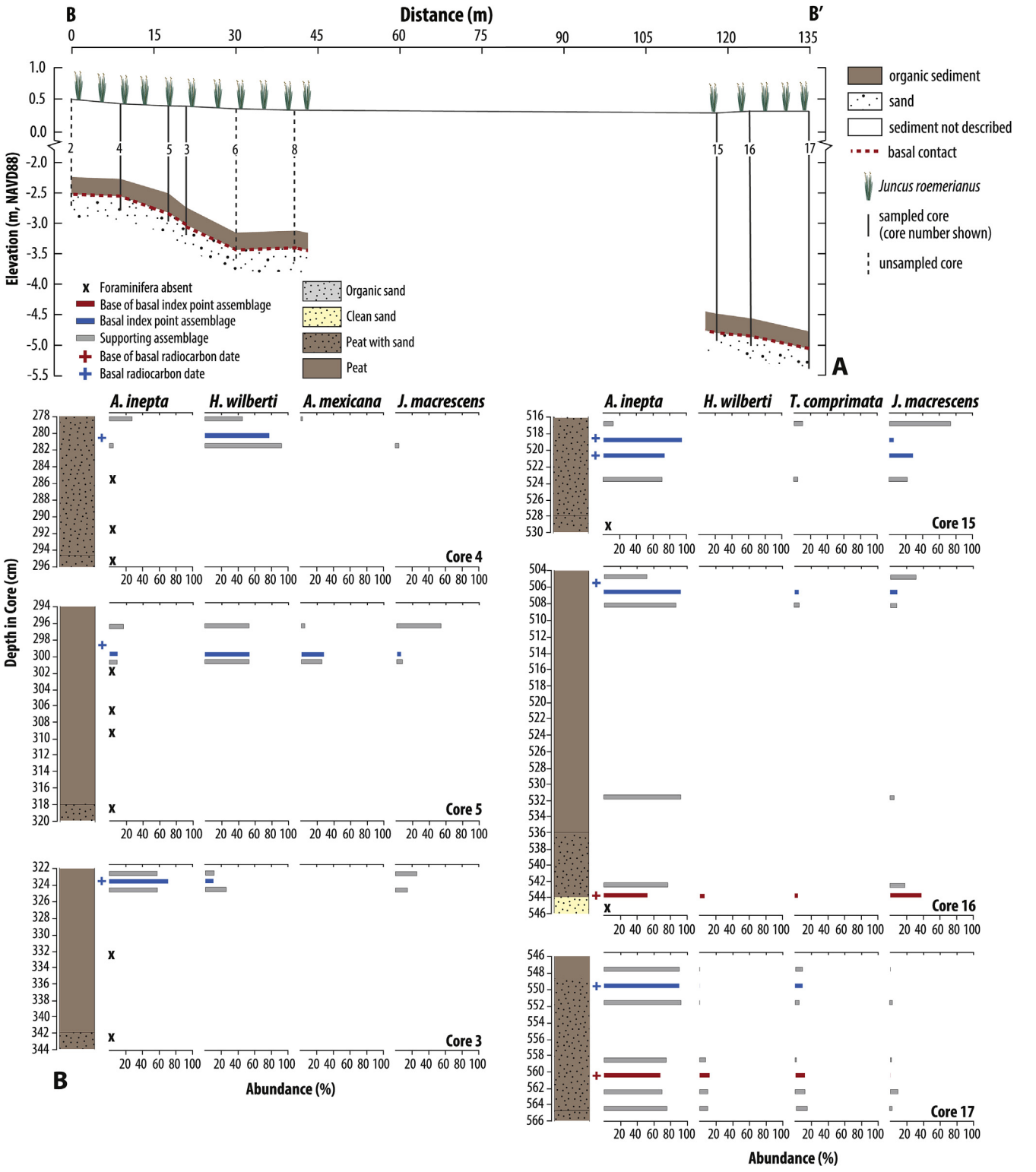

Fig. 4. Cores and samples used to develop sea-level index points along transect B–B′ at STM 2. **(A)** Position of sampled cores along transect B–B′ used to describe the contact between basal sand and the overlying organic units. **(B)** Lithology of individual cores and foraminifera enumerated from 1-cm thick samples, only the most common four species are shown. Colored bars represent the foraminiferal data used to infer the environment of deposition for producing sea-level index points. The position of radiocarbon-dated material is also shown. (For interpretation of the references to color in this figure legend, the reader is referred to the web version of this article.)

salt-marsh reconstructions. The ICE 6G-C VM6 model intersects with the St, Marys RSL reconstruction at 5.5 to 7.0 ka, after which it is considerably lower than the reconstruction. There are a limited number of regions with sea-level index points older than ~6.0 ka, but the nature of this discrepancy with the ICE 6G-C VM6 model is also noticeable in the Long Island, New Jersey, Outer Delaware, and northern North Carolina regions (see Fig. 15 of Roy and Peltier, 2015). The St. Marys RSL reconstruction suggests that there may

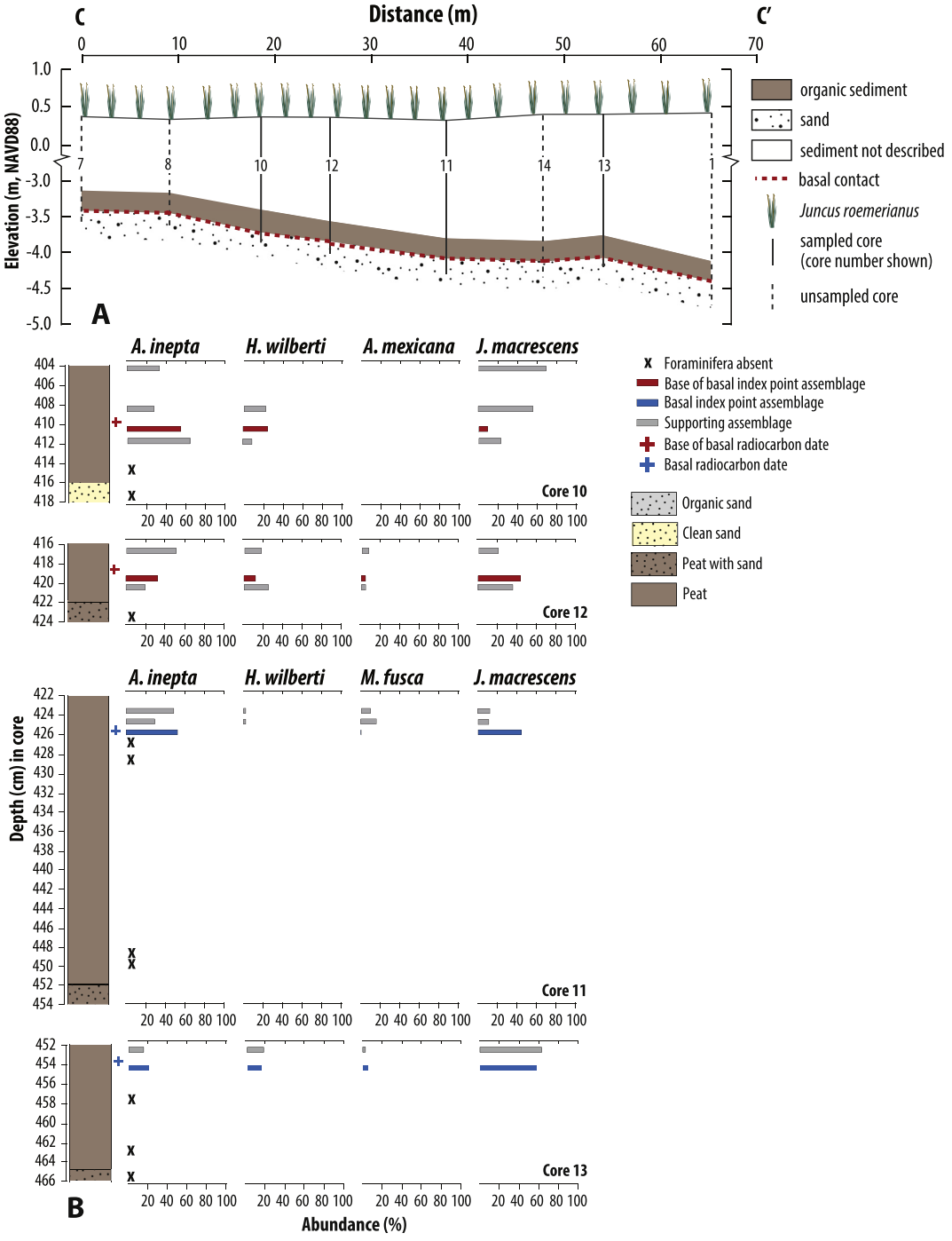

Fig. 5. Cores and samples used to develop sea-level index points along transect C–C′ at STM 2. **(A)** Position of sampled cores along transect C–C′ used to describe the contact between basal sand and the overlying organic units. **(B)** Lithology of individual cores and foraminifera enumerated from 1-cm thick samples, only the most common four species are shown. Colored bars represent the foraminiferal data used to infer the environment of deposition for producing sea-level index points. The position of radiocarbon-dated material is also shown. (For interpretation of the references to color in this figure legend, the reader is referred to the web version of this article.)

be a remaining misfit between RSL predictions and reconstructions particularly in the early to middle Holocene for regions located on the Laurentide Ice Sheet's collapsing forebulge. Lateral homogeneity of the mantle could be the cause of this remaining difference, as could contributions from processes such as sediment compaction and ocean dynamics that are not included in Earth-ice models (Roy and Peltier, 2015).

By expanding the database of Holocene sea-level index points to include northeastern Florida, our new reconstruction will help to provide an improved geographic link between U.S. Atlantic coast and Carribean databases of sea-level index points (Milne and Peros, 2013). The linked databases will support future efforts to establish the dynamic geometry of the collapsing forebulge throughout the Holocene by taking time slices of RSL data from a network of regions that incorporate near, intermediate, and farfield locations. Establishing the evolving size and position of the forebulge on continental scales is a robust test of Earth-ice models (e.g. Roy and Peltier, 2015) and will provide important insight (for example) into

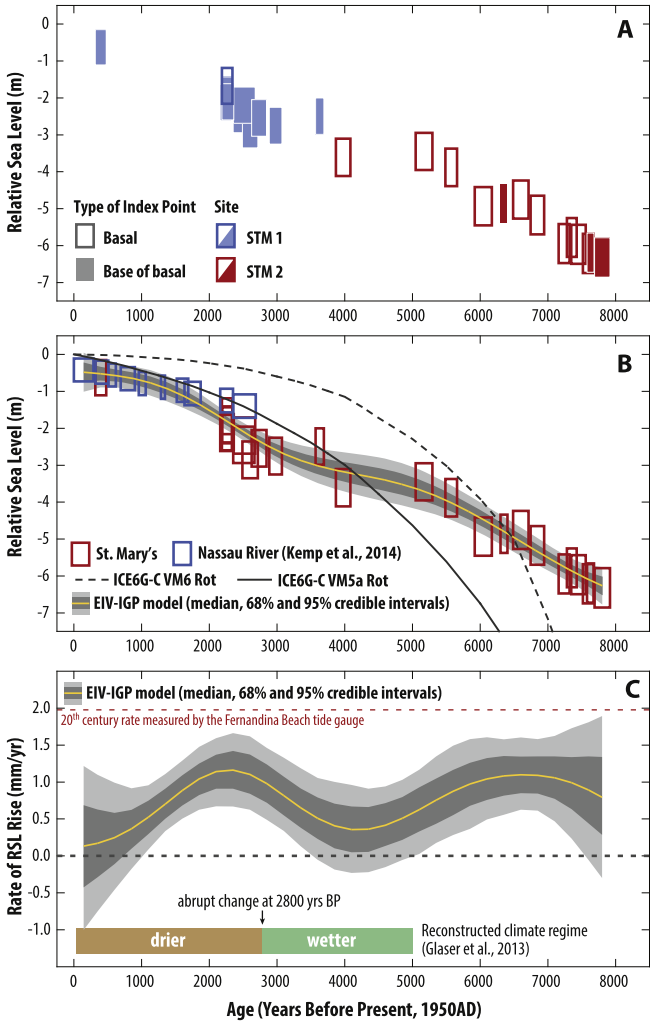

Fig. 6. Relative sea-level (RSL) reconstruction from northeastern Florida. **(A)** New sea-level index points developed from foraminifera preserved in radiocarbon-dated base-of-basal and basal salt-marsh sediment at the two St. Marys sites (STM 1 and STM 2). **(B)** Regional RSL history developed by combining standardized reconstructions from St. Marys with an existing dataset from the Nassau River estuary located ~15 km to the south (Kemp et al., 2014). An Error-in-Variables Integrated Gaussian Process (EIV-IGP) model was fitted to the RSL data to describe changes through time and to account for the temporal and vertical uncertainties in the data. RSL predictions developed for the St. Marys site from two Earth-ice models are shown for comparison. Both models use the ICE6G-C ice model and account for rotational feedback. The viscosity profiles (VM6 and VM5a) varies between the models. **(C)** Rates of RSL change estimated using the EIV-IGP model, positive values denote RSL rise. Periods of wetter and dry climate based on the climate reconstructions of Glaser et al. (2013). For comparison, the linear rate of RSL measured by the Fernandina Beach tide gauge for the period 1897–2014 is shown by a dashed labeled red line. (For interpretation of the references to color in this figure legend, the reader is referred to the web version of this article.)

research that aims to understand the driving mechanisms responsible for coastal geomorphic change on millennial timescales (e.g. Engelhart and Horton, 2011). Similarly, linking to other databases of sea-level index points (e.g. United Kingdom; Shennan and Horton, 2002) will further refine our understanding of three dimensional and time-dependent GIA processes.

5.2. Holocene sea-level highstand in Florida

The U.S. Atlantic coast database of Holocene sea-level index points demonstrated that there was no regional-scale RSL highstand at locations between Maine and southern South Carolina (Engelhart and Horton, 2012). However, a critical caveat to the discussion about the presence (or lack of) and nature of a mid-Holocene highstand along the U.S. Atlantic coast was the absence of valid sea-level index points from Florida and Georgia. At Key Biscayne in southeastern Florida, Froede (2002) proposed that a Holocene highstand of at least +0.5 m occurred at 1–2 ka based on the reinterpretation of fossilized root casts belonging to sub-tidal turtle grass rather than intertidal mangroves. On the northern Gulf coast of Florida, Donoghue and White (1995) inferred a small sea-level highstand in the late Holocene from seismic and archaeological evidence (a change in shell midden stratigraphy from open-estuarine molluscs and marine fish to brackish molluscs and fish that was interpreted as evidence for RSL fall) preserved on barrier islands. In southwest Florida, Stapor et al. (1991) used radiocarbon dating of barrier island advances and retreats to conclude that sea level may have reached +4 m at approximately 1–2 ka. These studies rely on sea-level indicators with poorly defined or undefined indicative meanings and/or that are difficult to date and stand in contrast to nearby records produced from mangrove sediment that do not support the presence of a RSL highstand in southern Florida (Scholl and Stuiver, 1967). The new reconstruction from St. Marys and Nassau Landing indicates that RSL did not exceed its present elevation over the past 8.0 ka and the distribution of sea-level index points through time precludes the reasonable possibility that one occurred during an interval for which no reconstruction was produced (Fig. 6).

5.3. Relative sea-level plateau at St. Marys

Our RSL reconstruction from northeastern Florida includes a plateau from approximately 5.0–3.0 ka when the rate of RSL rise slowed to a minimum of ~0.4 mm/yr (Fig. 6). This feature is unusual along the U.S. Atlantic coast where regional-scale compilations of sea-level index points typically show a gradual and continuous deceleration of RSL rise caused by the declining input of meltwater to the global ocean and a decaying rate of GIA. The plateau present in the new reconstruction from northeastern Florida stands in contrast to this pattern. There are two possible explanations for the RSL plateau and reduced rate of RSL rise reconstructed at St. Marys.

The reduced rate of RSL rise and its subsequent recovery are evidence of a regional-scale RSL trend that was previously unknown because of an absence of valid sea-level index points from Florida and Georgia in the U.S. Atlantic coast database. Archaeological remains (e.g. shell middens) and radiocarbon-dated terrestrial material (e.g. the remains of freshwater trees) from the coast of Georgia were interpreted by DePratter and Howard (1981) as evidence for a RSL lowstand of at least −3.0 m at 3.0–2.4 ka. Similar studies from South Carolina also utilized archaeological remains to reconstruct a RSL lowstand of similar timing and magnitude (e.g. Brooks et al., 1979). In a response to DePratter and Howard (1981), Belknap and Hine (1983) correctly argued that no indicative meaning could be reliably assigned to the archaeological remains since they are underpinned by assumptions about human behavior. Furthermore, they highlighted that radiocarbon-dated terrestrial material provides only freshwater limiting dates rather than valid sea-level index points. Therefore these archaeological and terrestrial data did not, and could not, provide a valid RSL reconstruction.

The plateau in the St. Marys RSL curve may alternatively be the result of significant contributions from local-scale processes. The most commonly discussed processes are sediment compaction and tidal-range change. It is unlikely that sediment compaction is the driver of the reconstructed RSL trend because the sea-level index points at St. Marys were exclusively produced from base of basal and basal sediment to avoid or minimize the effect of compaction (e.g. Bloom, 1964; Edwards, 2006; Horton and Shennan, 2009;

Törnqvist et al., 2008). Modeling of Holocene tides along the U.S. Atlantic coast shows that tidal range was largely unchanged at regional spatial scales during the last ~7.0 ka (Hill et al., 2011). The tidal range at 8.0 ka in northeastern Florida was up to twice as large as today. At 9.0 ka predictions of paleo bathymetry suggest that the St. Marys sites was not influenced by tides. However, the spatial resolution of this model does not preclude larger variability in tidal range at local scales. Modeling of paleo-tides at higher spatial resolution for St. Marys is difficult because the site is several kilometers upriver from a dynamic barrier island system that separates a lagoon characterized by changing configurations of salt-marsh platforms, sandy shoals and sinuous channels (Hill et al., 2011). These geomorphic characteristics make the site prone to local-scale tidal range change through time that cannot be adequately modeled without a more detailed understanding of paleogeography. A series of NOAA-operated tide gauges along the St. Marys River show that locations closer to (or in) the open lagoon (Roses Bluff, St. Marys, Chester, and Fernandina) have great diurnal tidal ranges of approximately 2.0 m (Fig. 1B). In contrast, the Crandall Street tide gauge located further upriver has a reduced great diurnal tidal range of 1.61 m. The St. Marys River study site currently lies in the ~10 km stretch of river where the tidal range is attenuated by ~0.4 m (20–25%). During the Holocene when RSL was lower, it is reasonable to assume that the study site was located relatively further from the open lagoon and was therefore characterized by a dampened tidal range compared to the contemporary site in the lagoon. In addition, dynamic geomorphic changes such as the building of barrier islands and/or the opening or closing of barrier island inlets could have altered the tidal prism for the entire lagoonal system, including the St. Marys River.

An additional local-scale factor that could influence the RSL reconstruction from St. Marys is the base level of freshwater flow in the river. In estuarine systems, the base flow of river discharge effects the extent to which tides can propagate up river (e.g. Friedrichs and Aubrey, 1994) and local tidal ranges (e.g. Jay et al., 2011). Higher base flow would attenuate tidal penetration and reduce tidal range, while lower base flow would enable greater penetration of tides upriver and result in larger tidal range. During the Holocene Florida experienced climate changes that resulted in alternating wetter and drier conditions. In the Florida Everglades, Glaser et al. (2013) reconstructed a period of unusual wetness from 4.6 to 2.8 ka that included more frequent tropical cyclones. If northeastern Florida received increased annual average precipitation during this period, then it is reasonable to presume that the base flow in the St. Marys River was correspondingly higher. The relative paucity of sea-level index points from St. Marys during the period from ~5.0 to 3.0 ka could indicate that higher base flow attenuated tidal penetration and consequently led to freshwater conditions prevailing at the study site for much of this interval. Although basal core samples from this period frequently lacked foraminifera, the presence of three sea-level index points indicate that there was at least episodic marine influence. Furthermore, if elevated and prolonged increase in baseflow reduced tidal range, then the reference water level that we assigned to core samples under the assumption of a constant tidal prism would be too high resulting in a RSL reconstruction that is too low (see Equation (1)). Therefore the apparent reduced rate of RSL rise could be partly explained by a change tidal range caused by increased river flow that we were unable to incorporate into our reconstruction. At 2.8 ka the Florida Everglades record an abrupt switch to a drier climate (Glaser et al., 2013), which is mirrored in paleoclimate reconstructions from the Caribbean (e.g. Hodell et al., 1991) and the Yucatan Peninsula (e.g. Hodell et al., 1995). If this drying of the climate was accompanied by reduced base flow in the St. Marys River, then it is conceivable that tides were able to more readily extend into the estuary resulting in the increased rate of RSL rise reconstructed between 3.0 and 2.0 ka and the greater density of sea-level index points (Fig. 6). This change would likely have been accompanied by an increase in tidal range.

6. Conclusion

We developed 25 new sea-level index points spanning the past ~8.0 ka in northeastern Florida. This reconstruction addresses the spatial gap in the U.S. Atlantic database which previously only extended from Maine to southern South Carolina and is also geographically important supporting efforts to link Holocene RSL reconstructions from North America and the Caribbean. The region is also of interest because it adds data to the spatially and temporally- variable GIA at the distal edge of the collapsing forebulge which is sensitive to forbulge geometry. This multi-millennial trend of RSL rise displays the characteristic pattern of collapse of the Laurentide Ice Sheet's proglacial forebulge and no evidence for the occurrence of a Holocene highstand. With the additional data from nearby Naussa River an EIV-IGP model identifies a RSL plateau between ~5.0–3.0 ka when the rate of RSL rise slows. It is not currently possible to determine if this is a regional signal. Local-scale processes including tidal-range change and/or trends in base flow of the St. Marys River driven by climate dynamics may have caused the plateau in RSL. We suggest that the plateau is unlikely due to compaction because the reconstruction is comprised of basal sea-level index points. RSL reconstructions provide empirical data to test Earth-ice models. The ICE-6G_C VM5a model shows good fit from ~4.0 ka to present, while the ICE-6G_C VM6 model fits over a short period in the earlier Holocene with RSL from St. Marys. However, discrepancy in model-reconstruction fit in the early to mid Holocene remain in northeast Florida and elsewhere along the Atlantic coast where records extend back into the early Holocene. The spatial validity of the St. Marys record requires supplementary RSL reconstructions (outside the St Marys River) at additional sites in Florida and Georgia, which will help to distinguish between contributions from local- and regional-scale processes.

Acknowledgements

This work was supported by National Oceanic And Atmospheric Administration Award NA11OAR4310101 and National Science Foundation Awards OCE-1154978 and OCE-1458921. We thank Stefan Talke for sharing his insight into paleotidal regimes and Glenn Milne for discussions of regional GIA. Richard Sullivan, Jim Cedeberg and Emmy Tsang helped with fieldwork. This is a contribution to PALSEA2 and IGCP Project 588 "*Preparing for Coastal Change*".

Appendix A. Supplementary data

Supplementary data related to this article can be found at http://dx.doi.org/10.1016/j.quascirev.2016.04.016.

References

Adams, D.A., 1963. Factors influencing vascular plant zonation in North Carolina Salt marshes. Ecology 44, 445.

Argus, D.F., Peltier, W.R., Drummond, R., Moore, A.W., 2014. The Antarctic component of postglacial rebound model ICE-6G_C (VM5a) based upon GPS positioning, exposure age dating of ice thicknesses and relative sea level histories. Geophys. J. Int. 198, 537–563.

Belknap, D.F., Hine, A.C., 1983. Evidence for a sea level lowstand between 4500 and 2400 years B.P. on the southeast coast of the United States; discussion and reply. J. Sediment. Petrol. 53, 680–685.

Bloom, A.L., 1964. Peat accumulation and compaction in Connecticut coastal marsh.

J. Sediment. Res. 34, 599–603.
Brooks, M.J., Colquhoun, D.J., Pardi, R.R., Newman, W.S., Abbott, W.H., 1979. Preliminary archaeological and geological evidence for Holocene sea level fluctuations in the lower Cooper River valley, South Carolina. Fla. Anthropol. 32, 85–103.
Cahill, N., Kemp, A.C., Horton, B.P., Parnell, A.C., 2015. Modeling sea-level change using errors-in-variables intergrated Gaussian processes. Ann. Appl. Stat. 9, 547–571.
Clark, J.A., Farrell, W.E., Peltier, W.R., 1978. Global changes in postglacial sea level: a numerical calculation. Quat. Res. 9, 265–287.
DePratter, C.B., Howard, J.D., 1981. Evidence for a sea level lowstand between 4500 and 2400 years B.P. on the southeast coast of the United States. J. Sediment. Res. 51, 1287–1295.
DePratter, C.B., Thompson, V.D., 2013. Past shorelines of the Georgia coast. In: Thompson, V.D., Thomas, D.H. (Eds.), Life Among the Tides – Recent Archaeology of the Georgia Bight. American Museum of Natural History, pp. 145–168.
Dey, D., Ghosh, S.K., Mallick, B.K., 2000. Generalized Linear Models: a Bayesian Perspective. CRC Press.
Donoghue, J.F., White, N.M., 1995. Late Holocene sea-level change and delta migration, Apalachicola River region, northwest Florida, U.S.A. J. Coast. Res. 11, 651–663.
Edwards, R.J., 2006. Mid- to late-Holocene relative sea-level change in southwest Britain and the influence of sediment compaction. Holocene 16, 575–587.
Edwards, R.J., Wright, A.J., 2015. Foraminifera. In: Shennan, I., Long, A.J., Horton, B.P. (Eds.), Handbook of Sea-level Research. John Wiley & Sons, pp. 191–217.
Engelhart, S.E., Horton, B.P., 2012. Holocene sea level database for the Atlantic coast of the United States. Quat. Sci. Rev. 54, 12–25.
Engelhart, S.E., Peltier, W.R., Horton, B.P., 2011. Holocene relative sea-level changes and glacial isostatic adjustment of the U.S. Atlantic coast. Geology 39, 751–754.
Farrell, W.E., Clark, J.A., 1976. On postglacial sea level. Geophys. J. R. Astron. Soc. 46, 647–667.
Friedrichs, C.T., Aubrey, D.G., 1994. Tidal propagation in strongly convergent channels. J. Geophys. Res. Oceans 99, 3321–3336 (1978–2012).
Froede, C.R., 2002. Rhizolith evidence in support of a late Holocene sea-level highstand at least 0.5 m higher than present at Key Biscayne, Florida. Geology 30, 203–206.
Glaser, P.H., Hansen, B.C.S., Donovan, J.J., Givnish, T.J., Stricker, C.A., Volin, J.C., 2013. Holocene dynamics of the Florida Everglades with respect to climate, dustfall, and tropical storms. Proc. Natl. Acad. Sci. 110, 17211–17216.
Goldstein, S.T., Frey, R.W., 1986. Salt marsh foraminifera, Sapelo Island Georgia. Senckenberg. marit. 18, 97–121.
Hall, G.F., Hill, D.F., Horton, B.P., Engelhart, S.E., Peltier, W.R., 2013. A high-resolution study of tides in the Delaware Bay: past conditions and future scenarios. Geophys. Res. Lett. 40, 338–342.
Hill, D.F., Griffiths, S.D., Peltier, W.R., Horton, B.P., Tornqvist, T.E., 2011. High-resolution numerical modeling of tides in the western Atlantic, Gulf of Mexico, and Caribbean Sea during the Holocene. J. Geophys. Res. 116.
Hodell, D.A., Curtis, J.H., Brenner, M., 1995. Possible role of climate in the collapse of Classic Maya civilization. Nature 375, 391–394.
Hodell, D.A., Curtis, J.H., Jones, G.A., Higuera-Gundy, A., Brenner, M., Binford, M.W., Dorsey, K.T., 1991. Reconstruction of Caribbean climate change over the past 10,500 years. Nature 352, 790–793.
Horton, B.P., Shennan, I., 2009. Compaction of Holocene strata and the implications for relative sealevel change on the east coast of England. Geology 37, 1083–1086.
Jay, D.A., Leffler, K., Degens, S., 2011. Long-term evolution of Columbia river tides. J. Waterw. Port Coast. Ocean Eng. 137, 182–191.
Johnson, D.S., York, H.H., 1915. The Relation of Plants to Tide-levels; a Study of Factors Affecting the Distribution of Marine Plants. Carnegie Institution of Washington, Washington D.C.
Kaye, C.A., Barghoorn, E.S., 1964. Late Quaternary sea-level change and crustal rise at Boston, Massachusetts, with notes on the autocompaction of peat. Geol. Soc. Am. Bull. 75, 63–80.
Kemp, A.C., Bernhardt, C.E., Horton, B.P., Vane, C.H., Peltier, W.R., Hawkes, A.D., Donnelly, J.P., Parnell, A.C., Cahill, N., 2014. Late Holocene sea- and land-level change on the U.S. southeastern Atlantic coast. Mar. Geol. 357, 90–100.
Kemp, A.C., Horton, B.P., Culver, S.J., 2009. Distribution of modern salt-marsh foraminifera in the Albemarle-Pamlico estuarine system of North Carolina, USA: implications for sea-level research. Mar. Micropaleontol. 72, 222–238.
Khan, N., Ashe, E., Shaw, T.A., Vacchi, M., Walker, J., Peltier, W.R., Kopp, R.E., Horton, B.P., 2015. Holocene relative sea-level changes from near-, intermediate-, and far-field locations. Curr. Clim. Change Rep. 1, 247–262.
Liu, J., Milne, G.A., Kopp, R.E., Clark, P.U., Shennan, I., 2016. Sea-level constraints on the amplitude and source distribution of Meltwater Pulse 1A. Nat. Geosci. 9, 130–134. http://dx.doi.org/10.1038/ngeo2616.
Mckee, K.L., Patrick, W.H., 1988. The relationship of smooth cordgrass (*Spartina alterniflora*) to tidal datums – a review. Estuaries 11, 143–151.
Milne, G.A., Peros, M., 2013. Data–model comparison of Holocene sea-level change in the circum-Caribbean region. Glob. Planet. Change 107, 119–131.
Mitrovica, J.X., Gomez, N., Morrow, E., Hay, C., Latychev, K., Tamisiea, M.E., 2011. On the robustness of predictions of sea level fingerprints. Geophys. J. Int. 187, 729–742.
Peltier, W.R., Argus, D.F., Drummond, R., 2015. Space geodesy constrains ice age terminal deglaciation: the global ICE-6G_C (VM5a) model. J. Geophys. Res. Solid Earth 120, 450–487. http://dx.doi.org/10.1002/2014JB011176.
Peltier, W.R., Tushingham, A.M., 1991. Influence of glacial isostatic adjustment on tide gauge measurements of secular sea level change. J. Geophys. Res. 96, 6779–6796.
Pomeroy, L.R., Wiegert, R.G., 1981. Ecology of a Salt Marsh. Springer-Verlag, New York, New York.
Rasmussen, C.E., Williams, C.I.K., 2005. Gaussian Processes for Machine Learning. Massachusetts Institue of Technology Press.
Redfield, A.C., 1972. Development of a New England salt marsh. Ecol. Monogr. 42, 201–237.
Reimer, P.J., Bard, E., Bayliss, A., Beck, J.W., Blackwell, P.G., Bronk Ramsey, C., Grootes, P.M., Guilderson, T.P., Haflidason, H., Hajdas, I., Hatté, C., Heaton, T.J., Hoffmann, D.L., Hogg, A.G., Hughen, K.A., Kaiser, K.F., Kromer, B., Manning, S.W., Niu, M., Reimer, R.W., Richards, D.A., Scott, E.M., Southon, J.R., Staff, R.A., Turney, C.S.M., van der Plicht, J., 2013. IntCal13 and Marine13 radiocarbon age calibration curves 0–50,000 Years cal BP. Radiocarbon 55.
Roy, K., Peltier, W.R., 2015. Glacial isostatic adjustment, relative sea level history and mantle viscosity: reconciling relative sea level model predictions for the U.S. East coast with geological constraints. Geophys. J. Int. 201, 1156–1181.
Scholl, D.W., Stuiver, M., 1967. Recent submergence of Southern Florida: a comparison with adjacent coasts and other eustatic data. Geol. Soc. Am. Bull. 78, 437–454.
Scott, D.B., Gayes, P.T., Collins, E.S., 1995. Mid-holocene precedent for a future rise in sea-level along the Atlantic Coast of North America. J. Coast. Res. 11, 615–622.
Scott, D.B., Medioli, F.S., 1978. Vertical zonations of marsh foraminifera as accurate indicators of former sea levels. Nature 272, 528–531.
Shennan, I., Horton, B., 2002. Holocene land-and sea-level changes in Great Britain. J. Quat. Sci. 17, 511–526.
Shennan, I., Long, A.J., Horton, B.P., 2015. Handbook of Sea-level Research. Wiley-Blackwell, p. 600.
Stapor, F.W., Mathews, T.D., Lindfors-Kearns, F.E., 1991. Barrier-Island progradation and Holocene sea-level history in southwest Florida. J. Coast. Res. 7, 815–838.
Toscano, M.A., Macintyre, I.G., 2003. Corrected western Atlantic sea-level surve for the last 11,000 years based on calibrated ^{14}C dates from *Acropora palmata* framework and intertidal mangrove peat. Coral Reefs 22, 257–270.
Törnqvist, T.E., Wallace, D.J., Storms, J.E.A., Wallinga, J., van Dam, R.L., Blaauw, M., Derksen, M.S., Klerks, C.J.W., Meijneken, C., Snijders, E.M.A., 2008. Mississippi Delta subsidence primarily caused by compaction of Holocene strata. Nat. Geosci. 1, 173–176.
Turck, J.A., Alexander, C.R., 2013. Coastal landscapes and their relationship to human settlement on the Georgia coast. In: Thompson, V.D., Thomas, D.H. (Eds.), Life Among the Tides – Recent Archaeology on the Georgia Bight. American Museum of Natural History, pp. 169–190.
Walton, W.R., 1952. Techniques for recognition of living foraminifera. Cushman Found. Foraminifer. Res. 3, 56–60.
Wanless, W.R., 1982. Sea level is rising – so what? J. Sediment. Petrol. 52, 1051–1054.
Wiegert, R.G., Freeman, B.J., 1990. Tidal Salt Marshes of the Southeastern Atlantic Coast: a Community Profile. Biological Report. United States Fish and Wildlife Service.
Woodroffe, S., Barlow, N.L.M., 2015. Reference water level and tidal datum. In: Shennan, I., Long, A.J., Horton, B.P. (Eds.), Handbook of Sea-level Research. Wiley-Blackwell, pp. 171–182.
Wright, A.J., Edwards, R.J., van de Plassche, O., 2011. Reassessing transfer-function performance in sea-level reconstruction based on benthic salt-marsh foraminifera from the Atlantic coast of NE North America. Mar. Micropaleontol. 81, 43–62.